

Gross morphological features of the bones of the forearm and manus in the Indian grey mongoose (*Herpestes edwardsii*)

ABSTRACT

The study on the anatomy of the mongoose to understand the lifestyle and behavior is on the way. Though research are done to address the anatomy of the body systems of the members of this Herpestidae family, studies are not yet available on the bones of the forearm and manus that assist locomotion, predation and are of evolutionary significance. This study was done on the carcass of Indian Grey mongoose that suffered natural death and referred by the Directorate of Forest and Wildlife, Puducherry. The carcasses after their postmortem examination were subjected for cold water maceration and their morphological features were recorded and compared with other carnivores to appreciate their morphological adaptations. We found that the radius was a long bone with a shaft and 2 extremities. It had four surfaces and two borders. The ulna was also long and its shaft presented three surfaces and three borders. These bones were present as two separate bones and were in close contact with each other for the entire length, except for the proximal and distal interosseus spaces. The radio-ulnar groove was wide and deep. The body of the olecranon process of ulna was bent with a remarkable tilt medially. The shafts of both radius and ulna were curved from above downwards and their volar surfaces were concave. The anconeal process was disc shaped and the semilunar notch of ulna was deeply concave. The bones of the manus included seven carpals arranged in two transverse rows, five metacarpals, five digits with three phalanges each except for the first digit. Proximal sesamoids were two in all the five digits.

Key words: Mongoose, radius, ulna, carpals, metacarpus, phalanges, proximal sesamoids

INTRODUCTION

Mongoose belong to the family Herpestidae. Mongoose hair is used for making different kinds of brushes, including painting and makeup brushes. In India, they are protected under Schedule II (Part II) of the Indian Wild life (Protection) Act, 1972 and Convention on International Trade in endangered species of Wild Fauna and Flora (CITES), with a complete ban on its commercial trade. Yet around 50,000 mongooses are killed by poachers every year. They have short legs and their movement resembles crawling. They are opportunistic carnivores. They have the ability to dig into the ground and to change their nest, but lacks climbing skills (Galvez-Lopez, 2021). It will feed on a huge variety of different foods and it does not matter if its living or dead such as Reptiles, tiny birds and mammals, amphibians, insects, worms and crabs. Some species on the other hand will supplement their meals with fruits, vegetables, roots, nuts and seeds. They have 5 digits in both limbs and the digits in the hindlimb are naked while those in the forelimb has hairs (Ewer, 1973; Walker, 1975). Its digits are supported with powerful claws that are non retractile and is used for digging and to capture prey. Scientific literature in this species *Herpestes edwardsii* and related species in Herpestidae

are on the morphology and morphometric aspects are upcoming and are available on the brain, spinal cord, third eyelid, liver and pancreas, tongue, skull, vertebral column, bones of the hind limb. However, studies have not been made yet on the bones of the forelimb especially of the forearm and manus that play an important role in its locomotion, defence and predation. This current study aim to report on the gross morphological features of the radius and ulna, carpals, metacarpals and digits in this short legged animals and to functionally correlate it with the canines and felines.

MATERIALS AND METHODS

This study was conducted in the Department of Veterinary Anatomy and Histology, Rajiv Gandhi Institute of Veterinary Education and Research, (RIVER) Puducherry. The cadaver of the Indian grey mongoose were from the Puducherry region. These animals after death were referred by the Department of Forest and Wildlife, Puducherry for their post mortem examination in the Department of Veterinary Pathology. The cadavers of those animals that suffered natural death were alone utilized. These were subjected to radiographic inspection of the bones and joints in the radiology Unit, Teaching Veterinary Clinical complex, RIVER. These cadavers were then carefully removed off their skin and muscles to the best possible extent by dissection and the bony remains were subjected to maceration without burying in water as recommended by (Soni et al., 2021) for smaller specimens and (Nayyar & Gatak, 2021; Savitri et al., 2023) for human cadavers. The bones were then brushed with a soft bristled tooth brush to make them clean and to get rid of any adhering remnants. They were finally washed thoroughly with running tap water to get rid of the residual chemicals and then air dried as recommended by (Aggarwal et al., 2016). These bones were then studied for their features before finishing with lacquer. Their morphological details were photographed using Nikon digital camera with 12x zoom.

RESULTS AND DISCUSSION:

The skeleton of the forearm in Indian Grey mongoose consisted of 2 long bones; radius and the ulna. The Manus region comprised of the carpus, metacarpus and the digits.

RADIUS:

The radius in Indian grey mongoose was rod shaped with a shaft and 2 extremities (proximal and distal). The radius was medial in position and crossed the ulna cranially along its length; both proximally and distally. The shaft was flattened craniocaudally, as well as curved from above downwards. Similar findings were reported by Palanisamy et al., (2018) in Indian wild cat and El-Ghazali and El-Behery, (2018) in rabbit. Contrarily, in cheetah the shafts of radius and ulna were relatively straight and slender, with poorly developed distal ends (Ohale and Groenewald, 2003). Similarly, El-Ghazali and El-Behery (2018) recorded that the shafts of radius and ulna were straight in cat. The radius had 4 surfaces; dorsal, medial, lateral and volar and 2 borders; medial and lateral. The medial border was smooth. The lateral border was rough in its distal half. The dorsal surface was smooth and convex while its volar surface was concave

from above downwards and rough in its proximal half. On the proximal part of the volar surface, close to its lateral border was noticed the bicipital tuberosity (Fig 1b), which was tubercular in appearance, as observed by Palanisamy et al, (2018) in Indian wild cat, whereas Tomar et al., (2018) reported that it was semilunar, quadrangular shaped in royal Bengal tiger.

In the present study, the radial tuberosity was distinct (Fig 1a) whereas, Sundaram et al., (2015) recorded an indistinct radial tuberosity in orange rumped agouti. The proximal extremity of radius was transversely widened and its articular fovea was oval in shape and articulated with the medial condyle of humerus. There was a central notch in the anterior border of the rim of the proximal articular fovea which is in agreement with the findings of Tomar et al. (2018) in tiger. Just medially and adjacent to the notch, was present the coronoid process that received the groove next to the medial condyle of humerus (Fig 3a). The posterior border of the rim had a convex articular facet that articulated with the radial notch of ulna that is consistent with the observations made by Evans (1993), Sreeranjini et al., (2014) in leopard, Lucy and Harshan (2014) and Tomar et al., (2018) in tiger. The proximal articular fovea of radius in mongoose, did not possess the ridge as in other animals. The volar surface of radius in its proximal half, meets the dorsal surface of ulna. In the distal half, the lateral surface of radius meets the dorsal surface of ulna.

The distal extremity of the radius was expanded (Fig 1a) and had a slightly concave ovoid form that is in agreement with the findings of Dyce et al., (2002) in carnivores, in which adduction, abduction & rotation are permitted to the ante-brachiocarpal joint in addition to the major movements of extension and flexion. In the distal articular surface of radius was the trochlea (Fig 3b) that articulated primarily with the radio-intermediate carpal and to a lesser extent with ulnar carpal. The lateral surface of the trochlea was slightly concave and formed the ulnar notch that articulated with the articular circumference of the distal end of ulna. Medial to the articulation, the radius was prolonged to form the styloid process (Fig 1), whose lateral surface formed part of the carpal articular surface, while its medial portion was nearly flattened for insertion of medial ligament of the elbow joint. These findings are in accordance with the observations made by Evans (1993) in dog, Ohale and Groenewald, (2003) in cheetah, Podhade, (2007) and Sreeranjini et al., (2014) in leopard and Shuvo et al., (2023) in hippopotamus. Contrarily, Sundaram et al., (2015) revealed that, in the Orange rumped agouti, the styloid process was on the lateral side of radius.

In the present study, the radius and ulna were present as two separate bones (Fig 1,2) as reported by Podhade, (2007) in leopard and Sundaram et al., (2015) in orange rumped agouti. They were in close contact with each other for the entire length, except for the proximal and distal interosseous spaces. Both these bones were fused in black Bengal goat (Siddiqui et al., 2008), Antelope (France, 2009), Chinkara (Jangir, 2010), Lion (Nzalak et al., 2010), Chital (Choudhury et al., 2020) and Blue bull (Rohlan et al., 2022). In dog, these two bones were attached to each other only at their ends (Miller, 2018).

ULNA :

The ulna was a long bone, massive and longer than radius, with a shaft and 2 extremities. It was located on the postero-lateral aspect of the radius distally. Its shaft was curved along its entire length from above downwards, non-prismatic, flattened from side to side and presented 3 surfaces dorsal, medial and lateral and 3 borders medial, lateral and volar (Fig 2). Contrarily, Sreeranjini et al., (2014) in leopard, Palanisamy et al., (2018) in Indian wild cat and Tomar et al., (2018) in tiger had reported that, the ulna was 2 sided in the proximal third, and 3 sided (prismatic) towards the distal 2/3rd.

In the Indian grey mongoose, the dorsal surface of ulna was narrow and articulated with the radius and presented a rough elongated, elevated margo interosseous which is in accordance with the findings of Lucy and Harshan (2014) in tiger. The medial surface was smooth. The lateral surface had the radio-ulnar groove, that extended from the semilunar notch along the entire lateral surface of the ulna. The medial and lateral borders were indistinct. The volar border was thick and free (Fig 2).

The proximal extremity of ulna had an olecranon process, anconeal process, the semilunar notch and facet for the humerus (Fig 3c). The body of the olecranon process was bent and presented a remarkable tilt medially. According to Rohlan et al., (2022), the olecranon process in blue bull was directed dorso-caudally. In this species, the olecranon process was grooved and presented 3 prominences namely 2 tubercles anteriorly and the olecranon tuber posteriorly, the latter formed the summit of the olecranon (Fig 2). Similar observations were reported by Palanisamy et al., (2018) in Indian wild cat and Sreeranjini et al., (2014) in leopard. The semilunar notch of ulna was deeply concave in the present study. It articulated with the humeral trochlea. The anconeal process was disc shaped and was situated just above the semilunar notch. The latter finding is concurrent with the statements of Evans (1993) in dog. The anconeal process was received into the olecranon fossa of the humerus when the elbow was extended. The groove in between the 2 condyles of the distal extremity of humerus, articulated with the semilunar notch above and coronoid process of radius below. Below the semilunar notch were present the medial and lateral coronoid processes, that enclosed the radial notch between them. This articulated with the articular circumference of the radius (Fig 3c), as in tiger (Lucy and Harshan, 2014), leopard (Sreeranjini et al., 2014) and in tiger (Tomar et al., 2018). The medial coronoid process was more prominent. The lateral surface of medial coronoid process and medial surface of lateral coronoid process articulated with the posterior convex articular surface of radius. The medial and lateral coronoid processes extended proximally their articular surfaces, to receive the respective condyles of the humerus.

The distal end of ulna had an oval convex facet medially, for articulation with the corresponding oval slightly concave articular fovea of radius and a pointed projection laterally, the styloid process. These are in concurrence with the reports of Evans (1993) in dog. The styloid process of ulna had a facet distally that articulated with the ulnar carpal, similar to the

observation made by Lucy and Harshan (2014) in tiger. The volar aspect of styloid process had a convex facet for accessory carpal. The articular area in the distal part of ulna, medial to the styloid process also articulated with the ulnar carpal (Fig 3d).

The proximal radio-ulnar articulation that involved the concave facet of ulna with the corresponding convex facet on radius should permit rotation movement, in this species. The distal pivotal joint with convex facet on ulna that articulated with the concave facet of radius, coordinated and supported the movement in the proximal end. The shafts of both radius and ulna were uniform in their thickness and were bound to each other along their entire length by interosseous ligament, except for a small proximal and distal interosseous space between them. This coincides with the statements of Rohlan et al., (2022) in blue bull. But, El-Ghazali and El-Behery (2018) in cat and Tomar et al., (2018) in tiger observed a narrow interosseous space along the whole length of the 2 bones. Fusion of ulna with radius, prohibit the movements of pronation and supination in the domestic mammals. (Dyce et al., 2002). In this study the proximal and distal pivotal joints between radius and ulna in mongoose should enable rotational movement as reported by Evans (1993) in dog. The radio-ulnar groove in the present study was wide and deep.

MANUS:

The skeleton of manus consisted of carpals, metacarpals, phalanges and sesamoids (Fig 4,5). The carpals were 7 bones arranged in 2 transverse rows. The proximal row had 3 carpals viz., a fused radio-intermediate carpal, ulnar carpal and accessory carpal from medial to lateral as reported by Evans (1993) in dog, Dyce et al., (2002) in carnivores and Nzalak et al., (2010) in lion. The distal row comprised of 4 small bones viz., the 1st, 2nd, 3rd and 4th carpals as reported by Evans (1993) in dog, Nzalak et al., (2010) in lion, Sundaram et al., (2015) in orange rumped agouti and El-Ghazali and El-Behery (2018) in cat. But it accounted 9 carpals in rabbit (El-Ghazali and El-Behery, 2018).

The radio-intermediate carpal was located on the medial aspect of the proximal row and was the largest of all carpals. It articulated proximally with the trochlea of radius, laterally with the ulnar carpal and distally with all the four carpals in the distal row. The smaller ulnar carpal articulated proximally with both radius and ulna, medially with the radio-intermediate carpal, on its palmar aspect with the accessory carpal and distally with the 4th carpal as well as with the metacarpal V. It possessed a small lateral process and a palmar process for articulation with accessory carpal and metacarpal V. These findings are consistent with the observations of Evans (1993) in dog. The accessory carpal had the shape of a truncated rod and presented a ventral projection at its free end. Similar morphology with a free thick overhang was reported by Miller (2018) in dog. The 1st carpal was the smallest of all carpals, nearly flattened, articulated proximally with radio-intermediate carpal, distally with metacarpal I and on its palmaro-medial aspect with the 2nd carpal and also with the base of the metacarpal II. The 2nd carpal was a dorso-ventrally compressed bone that articulated proximally with radio-intermediate carpal, distally

with metacarpal II, laterally with 3rd carpal and medially with 1st carpal. The 3rd carpal was larger than 2nd carpal with a distinct palmar projection, articulated proximally with radio-intermediate carpal, medially with 2nd carpal, laterally with 4th carpal and below with metacarpal III. The 4th carpal was the largest in the distal row. It was wedge shaped, articulated proximally with both radio-intermediate and ulnar carpal, medially with 3rd carpal and distally with metacarpal IV and V. A small spherical bone noticed on the medial side of the proximal end of the first metacarpal in the present study (Fig 4) was also recorded by Miller (2018) in dog, who stated that it was the smallest bone of the carpus located in the tendon of insertion of the muscle abductor digiti I longus.

METACARPUS:

There were five metacarpals which were cylindrical in shape and there was an increase in the thickness of the shaft of the metacarpals from first to the fifth (Fig 5). Each metacarpal consisted of a proximally enlarged base, a body or shaft and a distal part the head. The metacarpal I was the shortest. It articulated proximally with the 1st carpal and laterally with metacarpal II. Its distally present head articulated below with the proximal phalanx of the 1st digit & behind with a paired palmar sesamoid (Fig 5). The metacarpals II to V were the main metacarpals. The metacarpal III was the first longest, followed by the metacarpal IV, metacarpal II and metacarpal V as reported by El-Ghazali and El-Behery (2018) in rabbit and Sundaram et al., (2015) in orange rumped agouti. The metacarpals diverged distally and enclosed intermetacarpal spaces between them.

PHALANGES AND SESAMOIDS:

The forelimb consisted of 5 digits in this species, among which the first digit was rudimentary and the other four digits were fully developed. Each main digit consisted of a proximal, middle and a distal phalanx with 2 palmar proximal sesamoids at the metacarpophalangeal articulation (Fig 5). The proximal sesamoids articulated above with the head of the metacarpal and below with the palmar tubercles of the first phalanges. The first metacarpophalangeal joint also had two proximal sesamoids. Whereas El-Ghazali and El-Behery (2018) reported that the proximal sesamoid was absent in the first digit, in rabbit and cat. In this study the sesamoid were elongated as reported by El-Ghazali and El-Behery (2018) in cat. Further, they were slightly curved.

The first digit had only 2 phalanges that is in agreement with the findings of Sundaram et al., (2015) in orange rumped agouti. The middle phalanx was absent in the first digit in the present study. The size of the distal phalanx was as per the order of length of the metacarpals. The distal phalanx of the first digit was the shortest. Contrarily, Miller (2018) opined that the distal phalanges of all the four main digits were of the same size. In this species, all the five digits presented a prominent extensor process in the dorsal part of the distal phalanx. Miller

(2018) in dog reported that the extensor process were small and present only in the four main digits in dog. The distal part of the distal phalanges had unguis process that were in the form of a laterally compressed cone (Fig 5) and were covered by the horny claw. The unguis crest was seen as the bony shelf that encircled the dorsal and lateral parts of the base of this process as reported by Miller (2018) in dog. In the present study, the dorsal and distal sesamoids were not noticed as reported by El-Ghazali and El-Behery (2018) in cat.

CONCLUSION

In conclusion, most of these features in Indian grey mongoose are in common with other canines and felines and supported its adaptation for predation. These bones were relatively smaller and accounted for the shortness of the forelimb in this species. These morphological features could be extended in general to other species of this family Herpestidae.

Disclaimer (Artificial intelligence)

Author(s) hereby declare that NO generative AI technologies such as Large Language Models (ChatGPT, COPILOT, etc.) and text-to-image generators have been used during the writing or editing of this manuscript.

REFERENCE

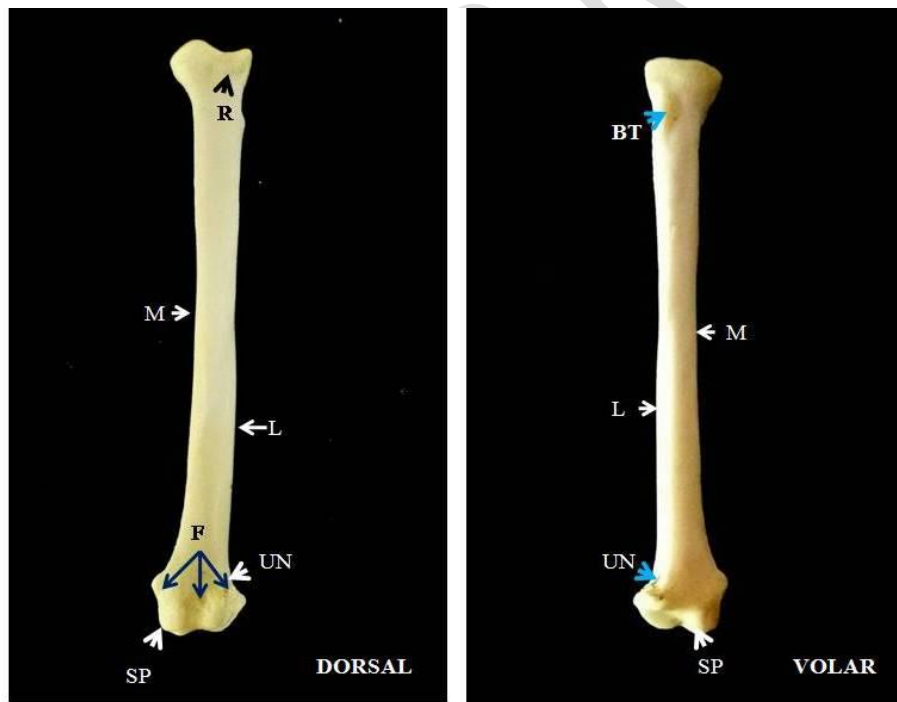
1. Aggarwal, N., Gupta, M., Goyal, P.M., Jaswinder Kaur J. (2016) An alternative approach to bone cleaning methods for anatomical purposes. *International Journal of Anatomy and Research*.4(2):2216-2221.
2. Choudhury, K.B., Dev, Deka, A., Rajkhowa, J., Sinha, S., Kachari, J. (2020) Comparative morphological studies on appendicular skeleton of arm of Asian palm civet (*Paradoxurushermaphroditus*) with domestic cat. *Journal of Entomology and Zoological Studies*, 8(4):1765-1767.
3. Dyce, K.M., Sack, W.O., and Wensing, C.J.G. (2002). *Textbook of Veterinary Anatomy*. Saunders-Elsevier Science, Philadelphia. 3rd ed. 840 pp.
4. El-Ghazali, H.M., and El-Behery, E.I. (2018). Comparative macroanatomical observations of the appendicular skeleton of New Zealand rabbit (*Oryctolagus cuniculus*) and domestic cat (*Felis domestica*) thoracic limb. *International Journal of Veterinary Science*, 7(3).127-133.
5. Evans, H.W. (1993) *Anatomy of the dog*. W.B. Saunders Co., Philadelphia, USA.
6. Ewer, R. F. (1973) *The Carnivores*. Ithaca, NY: Cornell University Press
7. France, D.L. 2009. *Human and Nonhuman Bone Identification, A Color Atlas*. CRC Press. Tyler and Francis Group.
8. Galvez-Lopez E. (2021) Quantifying morphological adaptations using direct measurements: The carnivoran appendicular skeleton as a case study. *The Anatomical Record*, 304, 480-506.

9. Jangir, D.K. (2010). Gross study on the bones of the forelimb in Indian gazelle (Gazelle gazelle bennetti). M.V.Sc thesis (Veterinary Anatomy and Histology), Rajasthan University of Veterinary and Animal Sciences, Bikaner.
10. Lucy, K.M., and Harshan, K.K. (2014) Gross Anatomy of skeleton antebrachii of a tiger (*Pantheratigris*). *Indian Journal of animal research*, 48(3):298-300.
11. Miller, M.E. (2018). The Anatomy of the dog. W.B. Saunders Co. Philadelphia, 5th edn, pp.64-78.
12. Nayyar, A.K., and Ghatak, S. (2021) Bone Preparation from Embalmed Human Cadavers - A Retrieval and Curation Technique. *Austin Journal of Anatomy*.8(1): 1098
13. Nzalak, J.O., Eki, M.M., Sulaiman, M.H., Umosen, A.D., Salami, S.O., Maidawa, S.M. and Ibe, C.S. (2010) Gross Anatomical studies on the bones of the thoracic limbs of the lion (*Pantheraleo*). *Journal of Veterinary Anatomy*, 3 (2): 65-71.
14. Ohale, L.O.C., and Groenewald, H.B. (2003) The morphological characteristics of the antebrachio carpal joint of the cheetah (*Acinonyxjubatus*). *Onderstepoort Journal of Veterinary Research*.70:15-20.
15. Palanisamy, D., Tomar, M.P.S., Ankem, P.B., Rao, D.S. and Ullakula, R.S., (2018) Macro-anatomy of radius and ulna in Indian wild cat (*Felislybicaornata*). *Indian Journal of Veterinary Anatomy*, 30(1):72-74.
16. Podhade, D. (2007) Studies on characteristic features of appendicular skeleton of leopard as an aid in wildlife forensic. M.V.Sc.thesis, JNKVV, Jabalpur.
17. Rohlan, K., Kumar, V., Shringi, N., Faran, N.K. and Gill, D. (2022) Gross anatomical study on radius-ulna bone of blue bull (*Boselaphustragocamelus*). *The Pharma Innovation Journal*.11(7S):3053-3056.
18. Savitri, R.C., Yakkundi, Matapathi, N., Talawar, V. (2023) A review of Bone Preparation Techniques for Anatomical Studies. *Journal of Ayurveda Integrated Medical Science*. 10:112-117. <http://dx.doi.org/10.21760/jaims.8.10.16>
19. Shuvo, M.J.H., Shuvo, R.I., Emran, A.A., Rahman, M.T., Robin, I.H., Hasan, M.A., Jahid, M.T., Hussan, M., and Rahman, S. (2023) Morphometric analysis of adult hippopotamus forelimb bones. *Bangladesh Journal of Veterinary Medicine*. 21(1):7-15.
20. Siddiqui, M.S.I., Khan, M.Z.I., Sarma, M., Islam, M.N. and Jahan, M.R. (2008). Macroanatomy of the bones of the limb of black Bengal goat (*Capra hircus*). *Bangladesh Journal of Veterinary Medicine*. 6(1):59-66.
21. Soni, A., Kumar, A., Sharma, A., and Vohra, H. (2021) Comparison of maceration techniques for retrieval of bones. *Journal of the Anatomical Society of India*. 70:93-6
22. Sreeranjini, A.R., Ashok, N., Raajani, C.V., Indu, V.R., Maya, S., Lucy, K.M. and Chungath, J.J. (2014) Gross Anatomical studies on the radius and ulna of leopard (*Pantherapardus*). *Indian Veterinary Journal*, 91 (11)24-26.
23. Sundaram, V., Dumas, N., Adogwa, A., Rao, S. and Nayak, S.B. (2015) Morphological studies of the forelimb skeleton of the orange rumped agouti. (*Dasyproctaleporina* Linnaeus, 1758). *Annual Research & Review in Biology*, 8(4):1-9.
24. Tomar, M.P.S., Taluja, J.S., Vaish, R., Shrivastav, A.B., and Sumbria, D. (2018) Gross anatomy of radius and ulna in Royal Bengal tiger (*Pantheratigris*). *Applied Biological Research*, 20(2):172-176.

25. Walker, E. (1975). Mammals of the World; 3rd Edition vol. 3. Baltimore, Maryland: Hopkins University Press.

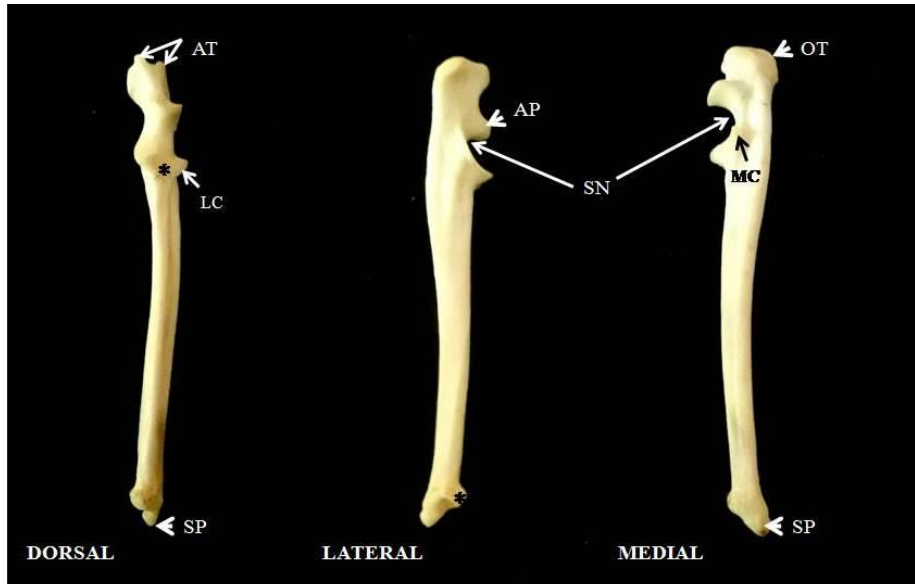
FIGURES:

Fig 1: Photograph of the left radius of mongoose showing its features in its dorsal and volar surface.



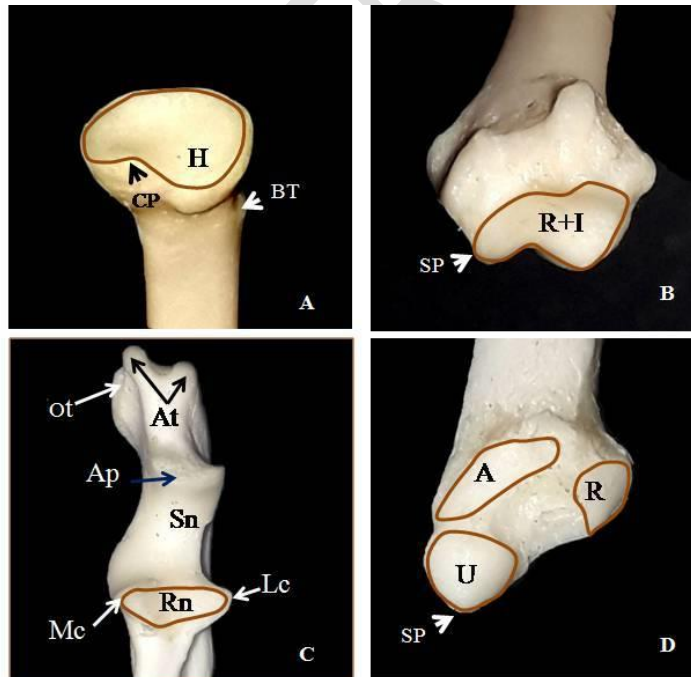
R- Radial tuberosity, M- Medial side, L- Lateral side, F- Fossa for extensors, UN- Ulnar Notch, SP- Styloid process, BT- Bicipital tuberosity.

Fig 2: Photograph of the left Ulna of mongoose showing its features in the dorsal, lateral and medial sides.



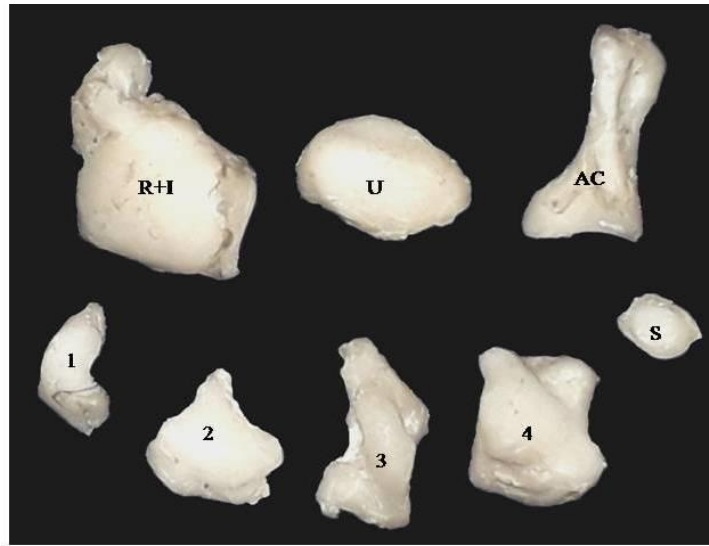
AT- Anterior tubercles of olecranon process, SP- Styloid process, AP- Anconeal process, SN- Semilunar Notch, OT- Olecranon tubercle, LC- Lateral coronoid process, MC- Medial coronoid process * Articular surface for radius (Radial Notch).

Fig 3: Photograph of the left proximal and distal extremities of the radius and Ulna showing its articular surfaces.



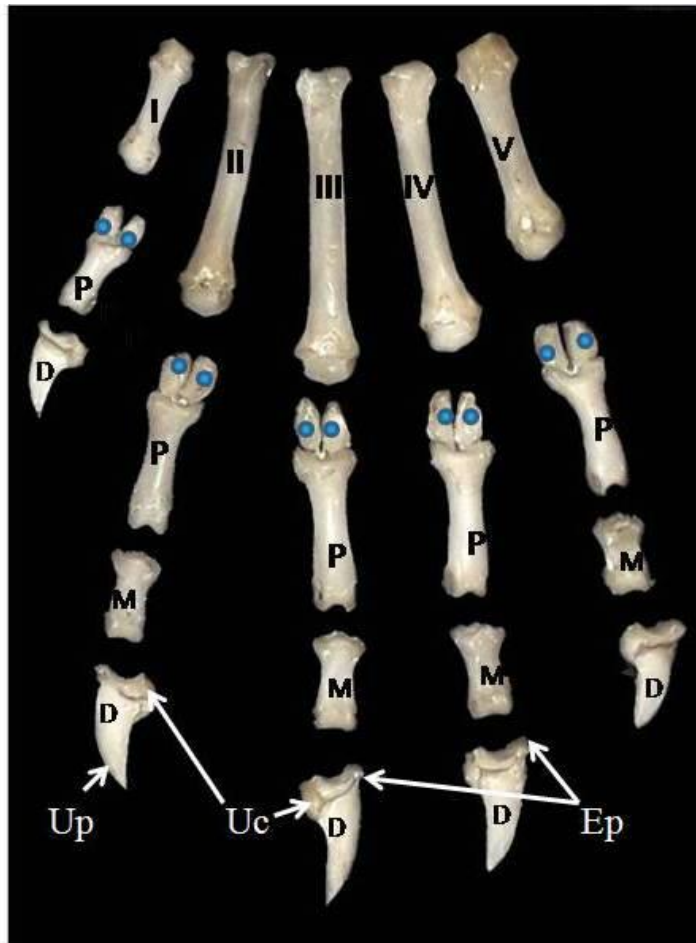
A- Proximal articular surface of Radius: H- Articular area for humerus, CP- Coranoid process, BT- Bicipital tuberosity . B- Distal articular surface of Radius: R+I- Articular surface for Radial+ Intermediate carpal, SP- Styloid process. C- Proximal articular surface of Ulna: At- Anterior tubercles, Ot- Olecranon tubercle, Ap- Anconeal process, Sn- Semilunar notch, Mc- Medial coronoid, Lc- Lateral coronoid process, Rn- Radial notch. D- Distal articular surface of Ulna: SP- styloid process, U- Articular surface for Ulnar carpal, A- for accessory carpal, R- Radius

Fig 4: Photograph of the proximal and distal row of carpal bones in mongoose showing its features.



R+I- Fused Radial and Intermediate carpal, U- Ulnar Carpal, AC- Accessary Carpal, S- Sesamoid, 1, First carpal, 2- Second carpal, 3- Third carpla, 4- Fourth carpal

Fig 5: Photograph of the Metacarpals and bones of the digits in mongoose showing its features.



I, II, III, IV, V- First, Second, Third, Fourth and Fifth Metacarpal bones, ● Proximal volar Sesmoid, P- Proximal Phalanges, M- Middle Phalanges, D- Distal Phalanges, Up- Ungual process, UC- Ungual crest, Ep- Extensor process